

Spatial mode switching in multi-user MIMO-OFDM systems: Performance in a real-world scenario

Malte Schellmann, Lars Thiele, Thomas Wirth, Volker Jungnickel, Thomas Haustein
 Fraunhofer Institute for Telecommunications, Heinrich Hertz Institute
 Einsteinufer 37, 10587 Berlin, Germany

{malte.schellmann, lars.thiele, thomas.wirth, volker.jungnickel, thomas.haustein}@hhi.fraunhofer.de

Abstract—Applying spatial mode switching in channel adaptive MIMO systems promises to achieve high spectral efficiencies in practical system setups. Several studies have pointed out significant performance gains obtained in realistically modeled channel scenarios. We have conducted channel measurements with the Berlin LTE-Advanced Testbed operated in the city center of Berlin and used these for the performance evaluation of a spatial mode switching concept that has previously been evaluated in a link- and system-level simulation environment. Results from measurements and simulations are shown to be in close correspondence.

I. INTRODUCTION

Channel adaptive transmission combined with multiple antenna technology (multiple-input multiple-output (MIMO)) is seen as a promising concept to achieve high spectral efficiencies in future radio networks [1]. While MIMO enables spatial multiplexing transmission of multiple data streams in the same frequency resource, the channel adaptive concept allows to form precoding vectors matched to the MIMO channel as well as to adapt the data rate to the current signal to interference and noise ratio (SINR) conditions. The basic idea of adaptivity is that the user terminals (UTs) provide feedback on their actual channel conditions to the base station (BS) [2]. This information is used at the BS within a resource allocation process to assign those transmission resources to the UTs that support high data rates.

For channel adaptive MIMO transmission, there are two options that enable boosting the achievable spectral efficiencies further: The first one is termed spatial mode switching, where the system may select the number of independent data streams that are transmitted simultaneously in the spatial domain of a given frequency resource [3], [4]. Reducing the number of spatial streams may be especially advantageous if the MIMO channel is ill-conditioned or if a user experiences low SNR conditions. The second option is the efficient application of multi-user MIMO (MU-MIMO), which allows to assign the simultaneously transmitted spatial streams to different users [5], in contrast to single-user MIMO (SU-MIMO), where all spatial streams are assigned to the same user. For an orthogonal frequency division multiplexing (OFDM) based MIMO system with fixed

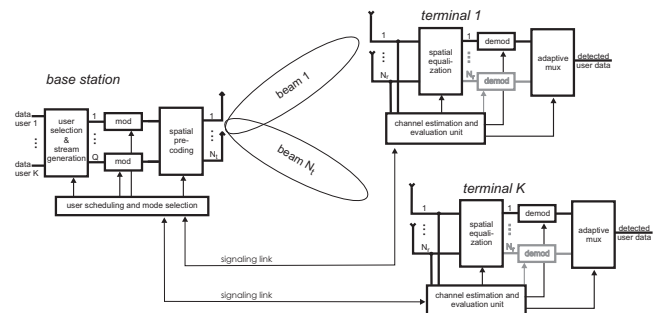


Fig. 1. System concept for channel-adaptive transmission in multi-user MIMO downlink.

precoding vectors, it has been shown in [6], [7] that proper application of MU-MIMO enables the efficient use of spatial multiplexing transmission even at low SNR conditions.

The performance of fixed precoding MIMO transmission supporting spatial mode switching in an OFDM system with a configuration similar to the 3G Long Term Evolution (LTE) specification has recently been evaluated in a link-level [6] as well as in a system-level environment [7]. While link-level simulations were based on the WINNER channel model (WIM) [8], system-level simulations were based on the spatial channel model extended (SCME) [9]. For both channel models, co-polarized MIMO antennas have been assumed. In this paper, we carry out similar investigations for real-world channels measured with the Berlin LTE-A Testbed for a 2×2 MIMO setup with cross-polarized MIMO antennas. Comparison of the obtained results with those from link- and system-level investigations reveals close correspondence.

II. SYSTEM CONCEPT

We consider the downlink of a broadband multi-user MIMO-OFDM system, where a BS with N_t antennas communicates with K UTs equipped with N_r antennas each (refer to Fig. 1). The BS provides $B \geq N_t$ fixed beams \mathbf{b}_u , which are used for spatial precoding of the transmission signals (grid of beams (GoB) concept, presented in [10]). Up to N_t beams may be simultaneously

served, each one being used to transmit an independent data stream. Adjusting the number of simultaneously served beams Q enables the system to support spatial transmission mode switching, where we distinguish between single-stream (ss) mode ($Q = 1$) and multi-stream (ms) mode ($2 \leq Q \leq N_t$).

Transmission is based on a radio frame structure, where each frame is constituted of several consecutive OFDM symbols. The total transmission resources of a radio frame are given by the subcarriers available for signal transmission. By subdividing the signal bandwidth into single subbands confined to a fixed number of consecutive subcarriers, we partition these transmission resources into resource blocks (RBs). The RBs form the basic scheduling resources that can be individually assigned to distinct users. Each RB is processed separately and thus may support an individual spatial transmission mode.

We assume a uniform transmit power allocation over all subcarriers; hence the transmission equation for each subcarrier signal is given by

$$\mathbf{r} = \mathbf{H}\mathbf{C}\mathbf{s} + \mathbf{n} \quad (1)$$

where \mathbf{H} is the $N_r \times N_t$ dimensional MIMO channel and \mathbf{C} is the $N_t \times Q$ precoding matrix comprising Q of the B beams \mathbf{b}_u with unitary property, which are simultaneously served. \mathbf{s} is the transmit vector containing the Q transmit symbols with constant transmit power $E[\mathbf{s}^H\mathbf{s}] = P_s$. Here, $E[\cdot]$ denotes the expectation operator and $(\cdot)^H$ the conjugate transpose operator. Finally, \mathbf{n} is the noise vector with N_r circularly symmetric complex Gaussian entries, and its covariance is given by $E[\mathbf{n}\mathbf{n}^H] = N_0 \cdot \mathbf{I}$, with \mathbf{I} representing the identity matrix and N_0 being the power of the additive white Gaussian noise (AWGN).

Based on the GoB, each UT evaluates in each RB the post-detection SINRs for the data streams transmitted via the beams $\mathbf{b}_u, u \in \{1, \dots, B\}$. The total transmit power P_s is distributed uniformly over the Q beams contained in \mathbf{C} . Assuming a linear receiver \mathbf{w}_u , the achievable post-detection SINR for the signal transmitted on u -th beam \mathbf{b}_u for any spatial transmission mode ($1 \leq Q \leq N_t$) can be determined according to

$$\text{SINR}(\mathbf{b}_u) = \frac{\|\mathbf{w}_u^H \mathbf{H} \mathbf{b}_u\|^2}{\mathbf{w}_u^H \mathbf{Z}_u \mathbf{w}_u}, \quad (2)$$

$$\mathbf{Z}_u = \sum_{j=1, j \neq u}^Q \mathbf{b}_j \mathbf{H} \mathbf{H}^H \mathbf{b}_j^H + \frac{QN_0}{P_s} \mathbf{I}$$

The maximum SINR is achieved by choosing \mathbf{w}_u according to the optimum combining solution [11]:

$$\mathbf{w}_u = \varepsilon \mathbf{Z}_u^{-1} \mathbf{H} \mathbf{b}_u \quad (3)$$

with scaling factor ε . Having evaluated the post-detection SINR for the different supported spatial modes, the UT feeds back this information to the BS.

A. Resource allocation and fair user selection

Resource allocation and selection of the proper spatial transmission mode is carried out by a score-based

scheduling process, whose detailed description is given in [6]. This process is briefly sketched as follows: By using a suitable SINR-to-rate mapping function, each SINR value determined by the UTs is transformed to an achievable rate per supported beam in the corresponding spatial mode. To enable a direct comparison of the single per-beam rates from different spatial modes, the per-stream rates of ms mode are weighted by a factor that accounts for the fewer power allocated to each ms beam due to the beam power allocation P_s/Q . In particular, the factor is chosen to Q . For each user, the (weighted) per-beam rates from all modes over all RBs are ranked by their quality, and corresponding scores are assigned. Mode selection and resource assignment is then done for each RB individually: Firstly, each beam available per transmission mode is assigned to the user providing minimum score for that beam. Thereafter, the mode is selected which comprises the minimum overall user score. In essence, in each RB the minimum score user decides on the spatial mode to choose, and all remaining beams are individually assigned to the user providing minimum score for the beam.

The objective of this score-based resource allocation process is to assign each user his best resources, and the decision on the spatial mode is taken under the premise of achieving a high throughput for each user. Clearly, the process is of heuristic nature, and hence the global scheduling target of assigning each user an equal amount of resources is achieved on average only or if the number of available resources tends to infinity. However, its convenient property for practical applications is its flexible utilization, as the set of resources can be defined over arbitrary dimensions (time/frequency/space). Thus, fairness can be established on a small time scale, e.g. even for the scheduling of resources contained within a single OFDM symbol.

III. MEASUREMENT SCENARIO

For the real-world investigations, channel measurements have been conducted with the Berlin LTE-A Testbed that has been set up in the city center of Berlin [12]. Configuration of the physical layer is chosen according to a tentative working assumption for LTE-A issued around November 2005, supporting a bandwidth of 20 MHz. For further details on the configuration of the testbed, refer to [13].

The downlink measurement was done with one BS and one UT, which was synchronized to the BSs. There was no interference from other BS. The scenario was a typical macro urban scenario with a mixture of LOS and NLOS and multipath propagation between buildings, see Fig. 2. The measurement area consists of a mix of office buildings, general residential area and is to the east adjoined by the Tiergarten park. The BS antenna was placed on top of the building of the TU-Berlin main building, above roof top, at a height of 37 m. The BS sector used was the 30° north-east sector. For the antenna setup, $N_t = 2$ transmit and $N_r = 2$ receive antennas were

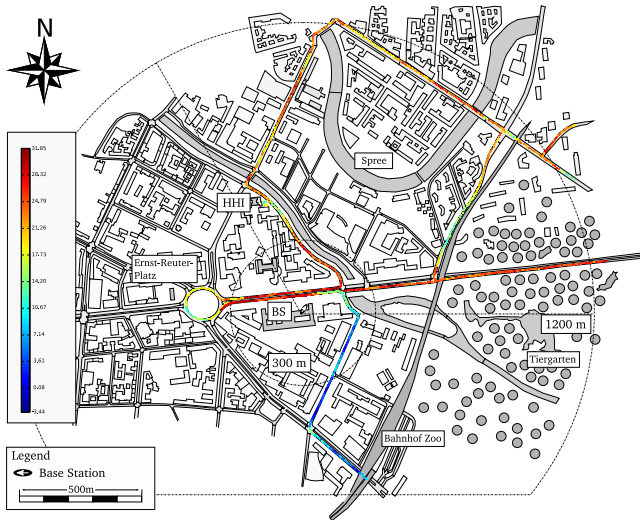


Fig. 2. Measurement scenario in macro urban environment in Berlin. Measurement track showing measured reception SNR (dB), averaged over receive antennas and transmission bandwidth.

used at the BS and UT, respectively. Both antenna sets were cross-polarized antennas ($\pm 45^\circ$). The BS antennas had a downtilt of 10° and an antenna gain of 18 dBi. The UT was placed in a car which moved at speeds of approximately 15-30 km/h on the measurement track. The measurement track is depicted in Fig. 2. The color-code corresponds to the measured SNR along the track. The outdoor test route covers a BS to UT distance ranging from 60 m to 1200 m.

For the analysis, we consider two special areas, marked on the map by the concentric circles. The first area is within the 300 m radius around the BS, which represents the cell center and will in the following be denoted as scenario 1. The second area covers the distances from 300 m to 1200 m, which is the outer cell annulus and will be referred to as scenario 2.

IV. RESULTS

In the following, results obtained from measurements will be compared with those from link- and system-level simulations, which are based on channels modeled with WIM and SCME, respectively. Fig. 3 shows the cumulative distribution functions (CDFs) of the reception SNR averaged over the receive antennas for the measured channels as well as for those modeled in an equivalent link-level scenario (WIM) and in a system-level scenario (SCME). Measurements were carried out at high SNR conditions; average measured SNR was 28.9 dB and 21.8 dB for scenario 1 and scenario 2, respectively. Hence, the channels could be recorded with high accuracy. For the evaluations here, artificial noise was introduced in order to achieve SNR conditions similar to those experienced in interference-limited multi-cell systems, which allows comparison to existing simulation results. This noise addition operation can be seen as an equivalent reduction of transmit power at the BS. In particular, SNR conditions were lowered by approximately 14.2 dB, yielding an

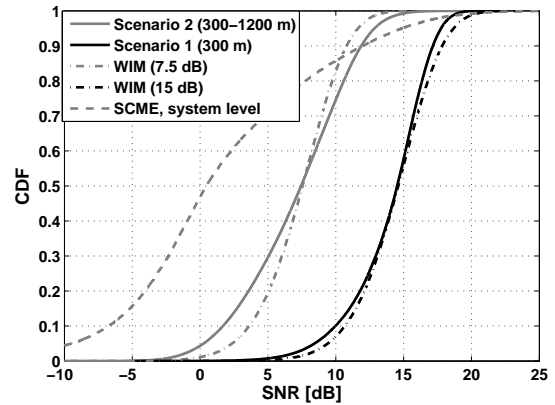


Fig. 3. CDFs of the SNR statistics for the different system setups.

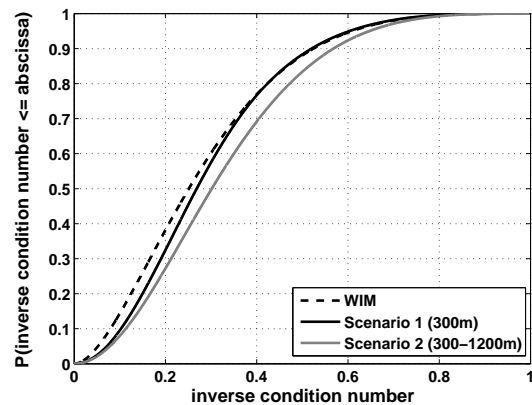


Fig. 4. CDF of the inverse channel condition number for WIM and measured channels.

average SNR of 14.7 dB for scenario 1 and 7.6 dB for scenario 2, respectively. Hence, we may compare the results for the two scenarios with results from an equivalent link-level scenario with average SNR of 15 dB and 7.5 dB, respectively. Fig. 3 reveals that the link-level statistics of WIM are very similar to those from the measured channels. For scenario 1, the corresponding CDFs are very close, while for scenario 2 larger deviations can be pointed out. This larger deviation for scenario 2 can be attributed to the wide range of distances considered (300-1200m), resulting in the fact that the path loss will have a non-negligible influence on the SNR statistics.¹ The CDF of SNRs from the SCME system level model shows a broad statistic with a mean SNR of 0.5 dB crossing the SNR curve of scenario 1 at around 11 dB. The broadening and the significant reduction of the mean SNR can be attributed to the presence of interference from adjacent cells.

To point out further differences between the conditions for measured and simulated channels, we also compare the statistics of the channel condition numbers. Fig. 4 depicts the CDFs of the inverse channel condition number

¹Note that the link-level investigations based on WIM consider only the small-scale fading effects of the channel, hence the path loss is neglected totally.

for the measured scenarios and simulated WIM channels. Note that a larger inverse channel condition number denotes a better conditioned channel. We observe that the measured channels exhibit slightly better channel conditions than those generated by the WIM. This can be attributed to the cross-polarized antennas used in the real-world setup, which enable the support of spatial multiplexing transmission even under strong LOS conditions (polarization multiplexing). We point out further that the inverse channel condition number increases with increasing distance to the BS, as can be seen by comparing the CDFs for scenario 1 and scenario 2. This can be attributed to the fact that the scattering resulting from object reflections becomes richer for increasing distance between BS and UT.

Next the spectral efficiency achievable after score-based scheduling will be determined for the two scenarios and compared to the corresponding link-level scenarios based on WIM. We assume two users to be randomly distributed in the cell service area, i.e. we randomly pick two measured channels from the scenario and carry out the channel evaluation and scheduling as presented in section II. As we have $N_t = 2$ transmit antennas here, only one ms mode with $Q = 2$ active streams is supported. The system thus may switch between ss mode ($Q = 1$) and dual-stream (ms) mode. The results are shown in Fig. 5 and 6 for scenario 1 and scenario 2, respectively. To point out the benefit of mode switching, we consider additionally a system configuration where the mode is fixed either to ss or to ms mode in both figures. Fig. 5 reveals that the CDFs for the three different transceiver configurations are quite similar for measured and modeled channels, yielding also similar gains from applying the spatial transmission mode switching. These results could be expected from the similar SNR distributions for measured and modeled channels shown in Fig. 3. However, the spectral efficiency for the ms mode is slightly higher for the measured channels, which can be related to the better channel conditioning (compare with Fig. 4): A better channel condition will clearly yield a smaller norm of the equalization vector \mathbf{w}_u in (3), and correspondingly the SINR achievable in ms mode will be higher. As a result, application of ms mode will be promoted in this case. In contrast to that, for the configuration where the mode is fixed to ss, we observe that the spectral efficiency for the measured channels is smaller than that for WIM channels. This can be related to the cross-polarized antennas being employed in the measurements, as these do not allow to achieve the beamforming gains realizable with co-polarized antennas, which have been assumed in WIM.

In scenario 2, relations are more different: First of all, we note that the CDF for the measured channels, especially for the adaptive and the fixed ms mode system, is much broader. This can be related to the path loss, which influences the SNR and SINR conditions additionally. However, most interestingly, we observe that the CDF of the adaptive system is closest to the CDF of pure

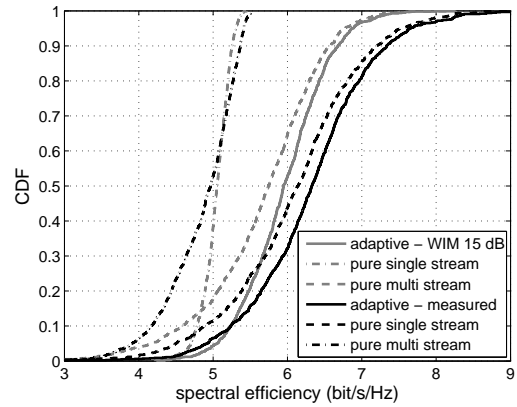


Fig. 5. Comparison of achievable spectral efficiency in the cell for measurements and WIM link-level simulations, $K = 2$ users. Scenario 1 – Cell center.

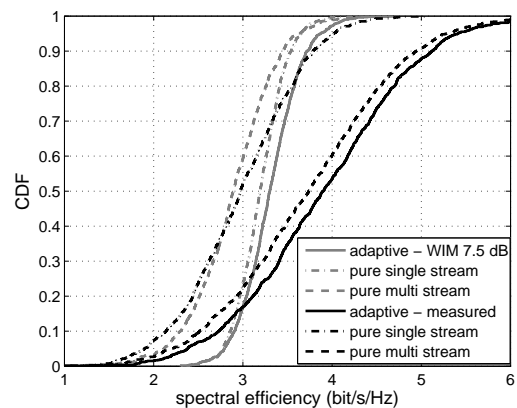


Fig. 6. Comparison of achievable spectral efficiency in the cell for measurements and WIM link-level simulations, $K = 2$ users. Scenario 2: Outer cell annulus.

ms mode for the measured channels, while for WIM channels the corresponding CDF is closest to the CDF of pure ss mode. Again, this can be attributed to the further improved conditioning of the measured channels (Fig. 4), promoting the application of ms mode.

The results from resource scheduling based on measured channels as well as the channels from link- and system-level simulations are finally compared in Table I, which comprises the probabilities of mode selection for ss and the two options for ms mode: MU-MIMO or SU-MIMO. Comparison of the results from measured scenario 1 with simulations based on WIM at 15 dB SNR

TABLE I
COMPARISON OF RESULTS FOR 2 ACTIVE USERS.

scenario	ss	ms		spectral eff. (bit/s/Hz)
		MU-MIMO	SU-MIMO	
scenario 1 link-level 15 dB	15.7 %	45.4 %	38.9 %	6.4
	23.5 %	37.6 %	38.9 %	6.0
scenario 2 link-level 7.5 dB	20.2 %	44.9 %	34.8 %	3.9
	50.2 %	34.1 %	15.7 %	3.3
system-level	27.1 %	43.7 %	29.2 %	2.7

(first row of table) reveals that the selection probabilities are very similar; however, the probability of MU-MIMO mode is slightly higher for measured scenario 1. Achievable spectral efficiencies are also quite close. In the second row, where results for scenario 2 are opposed to those from WIM at 7.5 dB SNR, we observe that now there are large differences in the selection probabilities. For evaluations based on WIM, selection of SU-MIMO is significantly decreased in favour of ss mode, while for the measured channels selection of SU-MIMO decreases only slightly. As already mentioned above, this can be attributed to the significantly better channel conditions in the measured scenario, which also yields a significantly improved spectral efficiency. It is interesting to note further that the probability to select MU-MIMO mode barely changes for scenario 1 and 2 as well as the corresponding cases based on WIM. This suggests that for a small number of users (i.e. when SU-MIMO is still frequently chosen), the decreased SNR conditions mainly affect the application of SU-MIMO mode, which complies to the famous finding concerning the tradeoff between spatial diversity and multiplexing in [14].

Finally, we also compare the results from system-level simulations based on SCME channel model. We observe that the selection probabilities are very similar to those for scenario 2, where users are distributed in the outer cell annulus. As the mean SNR of the system-level channel statistics is further decreased compared to scenario 2 (compare with Fig. 3), SU-MIMO mode is selected less frequently. However, note that the selection probability of MU-MIMO mode is nearly identical to that of scenario 1 and scenario 2. This observation substantiates the promotion of the MU-MIMO mode within the resource allocation process, which has already been pointed out in [6]. Moreover, it suggests that the selection probability for this mode becomes independent of the actual SNR conditions for the case of $K = 2$ users. The broader distribution of SNRs and its decreased mean value also result in a significantly decreased spectral efficiency of the multi-cell system, which amounts to 2.7 bit/s/Hz, emphasizing that inter-cell interference is the dominant performance limiting factor when going to a realistic multi-cell scenario.

V. CONCLUSION

The performance of the spatial mode switching concept for fixed precoding MIMO transmission introduced in [6] has been evaluated for real-world channels measured in the Berlin LTE-A Testbed. Results have been compared to those from link- and system-level investigations presented in [6], [7]. These investigations were based on channels modeled by the well-established broad-band MIMO models WIM [8] and SCME [9], respectively. While for the modeled channels co-polarized antennas were assumed, cross-polarized antennas have been used within the measurements. It has been shown that the SNR statistics of the link-level scenarios are close to those measured in real-world. Comparison of the channel

condition numbers revealed slightly better conditions for the measured channels, which can be attributed to the use of the cross-polarized antennas. Finally, the performance of spatial mode switching could be shown to be in close correspondence with the results from link- and system-level.

ACKNOWLEDGMENT

The authors wish to thank the German Ministry for Education and Research (BMBF) and Nokia Siemens Networks for financial support in the project ScaleNet.

REFERENCES

- [1] S. Catreux, V. Erceg, D. Gesbert, and J. Heath, R.W., "Adaptive modulation and MIMO coding for broadband wireless data networks," *Communications Magazine, IEEE*, vol. 40, no. 6, pp. 108–115, Jun. 2002.
- [2] D. Love, J. Heath, R.W., W. Santipach, and M. Honig, "What is the value of limited feedback for MIMO channels?" *Communications Magazine, IEEE*, vol. 42, no. 10, pp. 54–59, Oct. 2004.
- [3] R. Heath and A. J. Paulraj, "Switching between diversity and multiplexing in MIMO systems," *IEEE Trans. Commun.*, vol. 53, no. 6, Jun. 2005.
- [4] S. Chung, A. Lozano, H. Huang, A. Sutivong, and J. Cioffi, "Approaching the MIMO capacity with a low-rate feedback channel in V-BLAST," *EURASIP JASP*, no. 5, pp. 762–771, 2004.
- [5] M. Sharif and B. Hassibi, "On the capacity of MIMO broadcast channels with partial side information," *IEEE Trans. Inf. Theory*, vol. 51, no. 2, pp. 506–522, Feb. 2005.
- [6] M. Schellmann, L. Thiele, T. Haustein, and V. Jungnickel, "Spatial transmission mode switching in multi-user MIMO-OFDM systems with user fairness," *to appear in IEEE Transactions on Vehicular Technology*, 2009, preprint available at <http://www.mk.tu-berlin.de/mitarbeiter/hhi/wimi/schellmann>.
- [7] L. Thiele, M. Schellmann, T. Wirth, and V. Jungnickel, "Interference-Aware Scheduling in the Synchronous Cellular Multi-Antenna Downlink," *IEEE 69th Vehicular Technology Conference, VTC2009-Spring*, Apr. 2009, invited.
- [8] J. Salo, G. D. Galdo, J. Salmi, P. Kyösti, L. Hentilä *et al.*, "MATLAB implementation of the WINNER Phase I channel model," Dec. 2005. [Online]. Available: <https://www.ist-winner.org/3gpp-scm.html>
- [9] "3GPP spatial channel model extended (SCME)," May 2005. [Online]. Available: http://www.ist-winner.org/3gpp_scme.html
- [10] IST-2003-507581 WINNER – D2.7, "Assessment of advanced beam forming and MIMO technologies," Feb. 2005.
- [11] J. Winters, "Optimum combining in digital mobile radio with cochannel interference," *IEEE Trans. Veh. Technol.*, vol. 33, no. 3, pp. 144–155, Aug. 1984.
- [12] "Berlin LTE-Advanced testbed," <http://www.hhi.fraunhofer.de/bm>.
- [13] V. Jungnickel, M. Schellmann, L. Thiele, T. Wirth, T. Haustein *et al.*, "Interference-aware scheduling in the multiuser MIMO-OFDM downlink," *Communications Magazine, IEEE*, vol. 47, no. 6, pp. 56–66, Jun. 2009.
- [14] L. Zheng and D. Tse, "Diversity and multiplexing: a fundamental tradeoff in multiple-antenna channels," *IEEE Trans. Inf. Theory*, vol. 49, no. 5, pp. 1073–1096, May 2003.